

Cite this: *Energy Adv.*, 2026,  
5, 146Received 26th June 2025,  
Accepted 18th December 2025

DOI: 10.1039/d5ya00173k

rsc.li/energy-advances

## Comparative stability of the solid electrolyte interphase in potassium and sodium batteries

Jan Felix Schuster,<sup>a</sup> Le Anh Ma,<sup>a</sup> Christopher A. O'Keefe,<sup>b</sup> Clare P. Grey<sup>b</sup> and Reza Younesi<sup>\*,a</sup>

**Sodium-ion batteries (SIBs) and potassium-ion batteries (PIBs) are potential alternatives to lithium-ion batteries. However, knowledge about the solid electrolyte interphase (SEI) in SIBs and PIBs is still limited. Here, the formation and stability of SEI in SIBs and PIBs are compared to understand ageing related to SEI characteristics in electrolyte solutions based on 1 M KPF<sub>6</sub> or 1 M NaPF<sub>6</sub> in ethylene carbonate:diethyl carbonate (EC:DEC). Galvanostatic cycling coupled with pause testing was used to quantify the amount of charge consumed for electrolyte reduction for initial SEI formation and for SEI reformation required due to the dissolution of SEI. Proton nuclear magnetic resonance (<sup>1</sup>H-NMR) spectroscopy was used to reveal changes in the composition of electrolyte solutions due to SEI formation and dissolution. <sup>1</sup>H-NMR findings were supported by X-ray photoelectron spectroscopy (XPS) analysis showing the evolution of SEI composition during a 50 h pause.**

There is growing interest in sodium-ion batteries (SIBs) and potassium-ion batteries (PIBs) due to their potential to be more environmentally friendly and cheaper compared to lithium-ion batteries (LIBs).<sup>1</sup> To achieve this, the development of electrode and electrolyte materials based on abundant precursors and the establishment of a local supply chain is required. While the valuable knowledge and large volume of data from LIBs has helped in the development of SIBs, the further development of SIBs will benefit from a fresh look at potential electrode materials and electrolytes. There are numerous materials discarded for use in LIBs due to their incompatibilities with graphite or water-based coatings, which might be usable for SIBs.

The solid electrolyte interphase (SEI) has been shown to play a key role in the efficiency and cycling performance of LIBs and therefore a variety of work has been done to optimize the formation of stability of the SEI in LIBs.<sup>2</sup> The SEIs formed in

SIBs and PIBs are known to be inferior to their lithium counterpart and only a limited number of studies have been carried out to explore the similarities and differences of the SEI in SIBs and PIBs compared to that in LIBs.<sup>3,4</sup>

The understanding and design of a suitable electrolyte system in sodium and potassium batteries is a challenge that requires further understanding of the solvation structure of electrolyte solutions based on sodium and potassium. An ideal SEI is formed in the initial discharge/charge cycle and should be electronically insulating and impermeable to solvent molecules to prevent further electrolyte reduction. Further, it should have a high ionic conductivity to allow the migration of the respective alkali-ions. In addition, the SEI should be chemically stable and insoluble in the electrolyte to avoid additional capacity losses.<sup>5,6</sup>

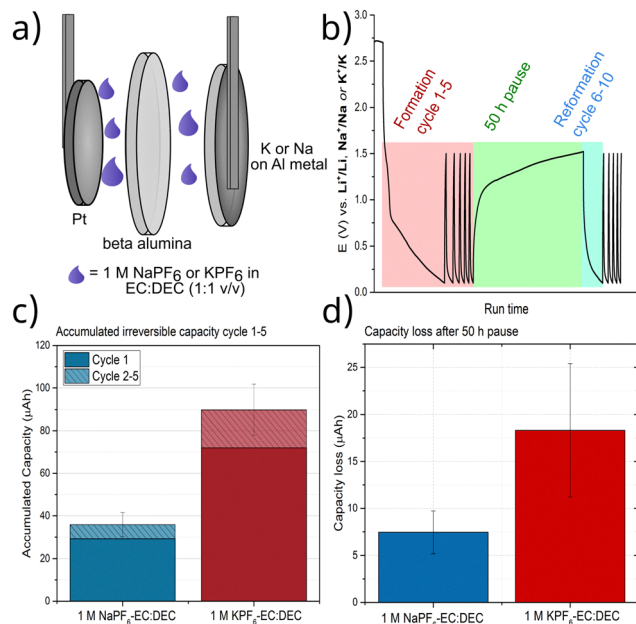
Herein, we investigate a simple 1 M NaPF<sub>6</sub>/KPF<sub>6</sub> EC:DEC (1:1 v/v) electrolyte with no additives. The goal was to gain understanding of the solvent stability and SEI formation. Galvanostatic cycling experiments coupled with pauses at open-circuit voltage (OCV) provide insight into the irreversible reduction capacity required for the formation and reformation of the SEI layer. Proton nuclear magnetic resonance (<sup>1</sup>H-NMR) spectroscopy was used to identify changes in the electrolyte composition due to dissolution of SEI species, while X-ray photoelectron spectroscopy (XPS) was employed to analyse changes in the SEI composition that happen during the extended pause at OCV.

Fig. 1a and b illustrates the schematic of the cell setup, and the galvanostatic cycling protocol used here to study the SEI stability in Na- and K-based electrolyte systems, *i.e.* 1 M NaPF<sub>6</sub> or KPF<sub>6</sub> in EC:DEC. Platinum foil was used as the working electrode to investigate the electrolyte reduction, SEI formation, and self-discharge during open circuit pause, in the absence of any mechanisms related to ion intercalations (*e.g.* ion trapping and volume expansion contributions), as discussed in a previous work.<sup>3</sup> Although Pt may exhibit catalytic effects on electrolyte reduction,<sup>7</sup> using Pt for both systems enables a valid comparison of SEI formation and dissolution without

<sup>a</sup> Department of Chemistry-Ångström Laboratory, Uppsala University, 75121 Uppsala, Sweden. E-mail: reza.younesi@kemi.uu.se

<sup>b</sup> Yusuf Hamied Department of Chemistry, University of Cambridge Lensfield Road, Cambridge CB2 1EW, UK





**Fig. 1** (a) Schematic of the cell setup to study formation and dissolution of SEI formed in 1 M NaPF<sub>6</sub> or 1 M KPF<sub>6</sub> in EC:DEC (1:1, v/v) electrolyte solutions. Note that a  $\beta$ -alumina membrane was utilized to eliminate crosstalk effects between the electrodes. (b) Galvanostatic cycling and pause test protocol. (c) Accumulated irreversible capacity (difference of reduction and oxidation capacity) of cycle 1 and cycles 2 to 5 indicating the charge consumed for SEI formation and reformation. (d) Capacity loss after 50 h of open circuit relaxation.

interference from intercalation processes. There is a clear difference in the potential applied to the model system depending on the electrolyte and alkali ion. The reduction potential of potassium is lower than that of lithium ( $-0.15$  V vs. Li<sup>+</sup>/Li (in EC:DEC)).<sup>8</sup> However, since carbonaceous anodes in practical potassium- and sodium-ion batteries operate at low potentials relative to their respective metal references, a constant low potential of  $0.1$  V vs. K or Na metal was applied to mimic realistic operating conditions. Although the potential difference may influence the SEI dissolution, we employ  $0.1$  V vs. K or Na metal as a reference to investigate this ageing mechanism within the voltage range relevant to full-cells operation. It is important to note that this is one essential part of the model cell to test the stability of the SEI under conditions that closely resemble a real cell setup. The aim is to compare the final SEI in both systems, not to compare SEI formed at the same absolute potential which would require a suitable reference and counter electrodes that remain stable in all systems. A beta alumina separator was used to inhibit any cross talk as this is known to influence the observed SEI formation in sodium and potassium systems.<sup>6,9,10</sup> The lower cut-off potential was chosen to be  $0.1$  V to avoid underpotential deposition of alkali metals, and therefore to only focus on the electrolyte reduction. The initial SEI formation (*i.e.* 1st reduction) consumed about  $29$   $\mu$ Ah and  $72$   $\mu$ Ah for the Na and K systems, respectively (see Fig. 1c). The higher amount of charge consumed for SEI formation in the K system compared to that in the Na system

reveals lower efficiency of 1 M KPF<sub>6</sub> in EC:DEC electrolyte compared to 1 M NaPF<sub>6</sub> in EC:DEC in forming a passivating SEI. The following cycles (reduction in cycle 2 to 5) show that there is some more charge consumed during reduction in each cycle. The reduction capacities measured between cycles 2 and 5 are likely dominated by contributions from leakage current and by the charge required to reform the SEI, which partially dissolves during cycling. The accumulated amount of charge consumed during cycle 2 to 5 was equal to  $6$  and  $12$   $\mu$ Ah for the Na and K, respectively (see Fig. 1c). As expected, this contribution is lower compared to the initial formation because the Pt electrode is largely passivated during the 1st reduction. However, the higher amount of charge consumed in cycle 2 to 5 for the K system compared to that in Na system, again indicates that the SEI in the K-cells is less efficient than that in Na-cells.

After 5 cycles, the passivated Pt electrode was relaxed at open circuit potential for 50 h and was then further reduced in a follow up reduction (see Fig. 1b). The reduction capacity after the 50 h rest reveals a continuously dissolving SEI during relaxation, requiring more capacity to reform the SEI. The reduction capacity after 50 h relaxation was almost twice as much in K system compared to that in Na system, *i.e.*  $18$   $\mu$ Ah vs.  $7$   $\mu$ Ah respectively, see Fig. 1d.

To identify dissolved SEI species, <sup>1</sup>H-NMR analysis was performed on pristine and extracted electrolytes from cells at the three different states: (i) as-assembled, (ii) 5 cycles, and (iii) after a subsequent 50 h pause. The expected signals of the EC (singlet at  $4.5$  ppm) and DEC (quartet at  $4.1$  and triplet at  $1.2$  ppm) were observed, see Fig. 2 and 3. Based on the integration of the signals in the <sup>1</sup>H NMR spectra, the ratio between the EC and DEC is different for the electrolytes at different states, see Fig. S1.

From pristine to being assembled, the relative concentration of DEC decreases significantly (about 50%) compared to EC. This is likely because of the evaporation of DEC due to the vacuum applied during the cell assembly. After cycling, both Na and K electrolyte systems show a lower ratio of EC to DEC compared to electrolytes at the assembly stage, indicating more EC is being reduced than DEC during cell cycling. However, the decrease in EC to DEC ratio is more significant in 1 M KPF<sub>6</sub>-EC:DEC electrolyte, which could correspond to a higher

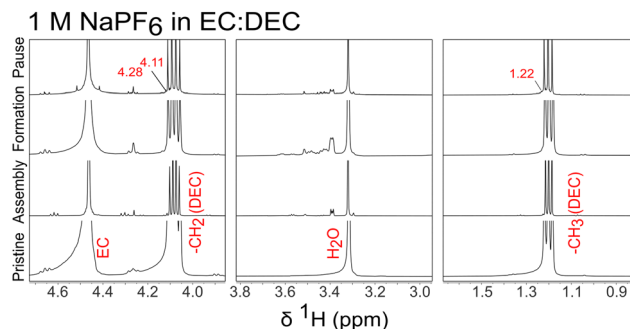


**Fig. 2** <sup>1</sup>H-NMR spectra of 1 M NaPF<sub>6</sub> in EC:DEC in the pristine, assembled, formation and after subsequent 50 h relaxation states. The spectra are normalized to the EC peak.



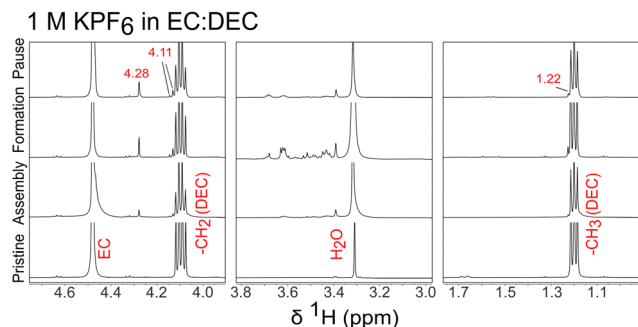


Fig. 3  $^1\text{H}$ -NMR spectra of 1 M  $\text{KPF}_6$  in EC:DEC in the pristine, assembled, formation and after subsequent 50 h relaxation states. The spectra are normalized to the EC peak.

amount of EC reduction during cycling in the potassium-based electrolyte compared to that in the sodium-based electrolyte.

After the 50 h relaxation at open circuit potential, the EC to DEC ratio remains almost unchanged in 1 M  $\text{NaPF}_6$ -EC:DEC electrolyte, while it increases in 1 M  $\text{KPF}_6$ -EC:DEC electrolyte. This reveals that more DEC is reduced during the 50 h pause indicating that the SEI formed in K-based electrolyte is not fully passivating leading to a reduction of more DEC during relaxation where no external current or potential is applied.

The major degradation products dissolved from the SEI formation are ethylene di-carbonate ( $\text{C}_4\text{H}_4(\text{Na/K})_2\text{O}_6$ ) and diethyl 2,5-dioxahexanedioate ( $\text{C}_6\text{H}_{10}\text{O}_6$ ). Both degradation products share the same singlet at 4.28 ppm (s). The singlet at 4.28 (Fig. 2 and 3) is assigned to (K/Na) ethylene di-carbonate.<sup>11,12</sup> Diethyl 2,5-dioxahexanedioate also has two signals seen as

shoulders at 4.11 and 1.24 (Na)/1.22 (K) ppm highlighted in red numbers in Fig. 2 and 3. Hofmann *et al.*<sup>13</sup> identified diethyl 2,5-dioxahexanedioate as a degradation product when leaving potassium metal in EC:DEC solution at 40 °C for 60 days. In deuterated acetonitrile, the signals were reported at 4.32 (s), 4.16 (q) and at 1.30 (t) ppm.<sup>13</sup> There are additional peaks of degradation and dissolution products from 3.3–3.6 ppm next to the 3.32 ppm singlet of the water impurity in the DMSO- $d_6$  solvent. Peaks around this area are typically assigned to PEO like oligomers.<sup>14</sup>

The NMR spectra of both systems look very similar in terms of peaks and their intensity. However, in the K-system, there are minor additional peaks from 1.5–1.7 ppm ( $^1\text{H}$  NMR) and at higher chemical shifts 6.5–7.2 ppm, which originate from protons in the same molecule/ion based on diffusion ordered spectroscopy (DOSY) measurements (Fig. S3). Hydrogen peaks from 6.5–7.2 ppm can be attributed to alkenes or aromatic peaks. It is not clear if these peaks belong to species that electrochemically formed or impurities reacting in the cell. The additional peaks observed in the formation and pause cell are also observed when checking calendar aged (2 and 4 weeks old) electrolyte samples (Fig. S4). It is not possible to assign these species due to their low concentration and peak overlap. Based on the different diffusion times estimated in the DOSY experiment (Fig. S3) these peaks belong to three decomposition species.

The SEI composition was further analysed by XPS using two different photon energies to probe different depths, as shown in Fig. 4. Based on the C 1s, a relatively higher concentration of carbonate and carboxyl species compared to hydrocarbon

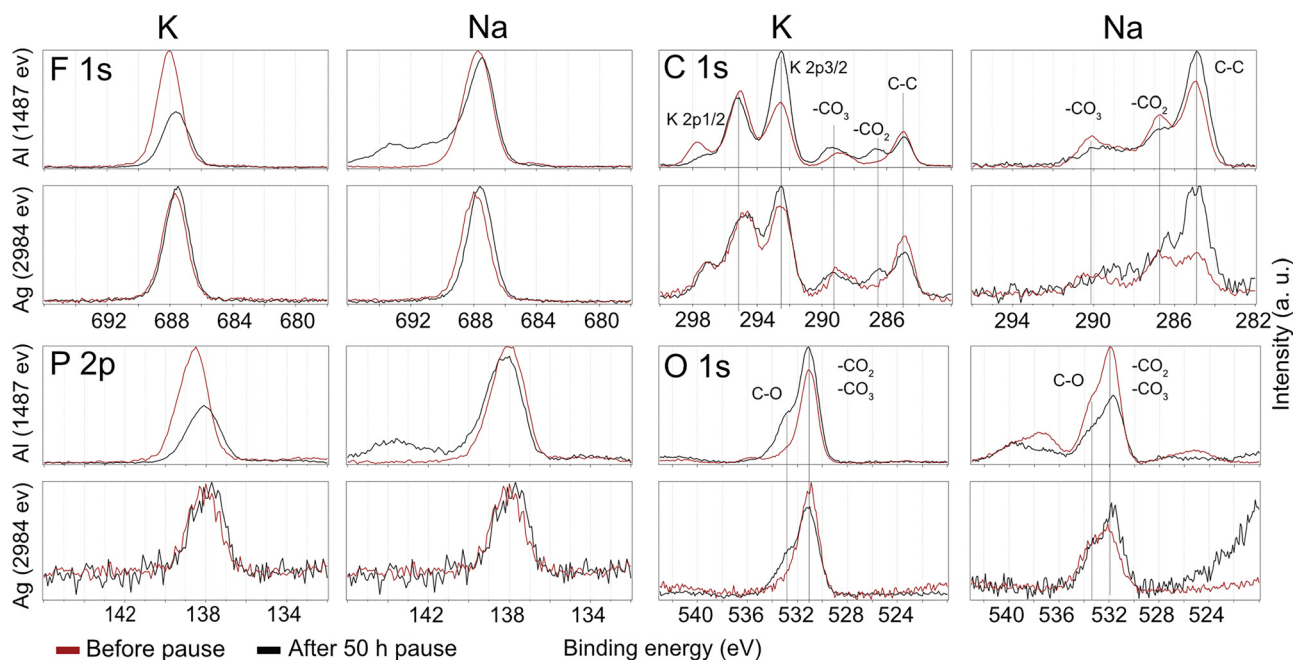


Fig. 4 F 1s, O 1s, P 2p, and C 1s XPS spectra of SEI formed in 1 M  $\text{KPF}_6$  in EC:DEC and 1 M  $\text{NaPF}_6$  in EC:DEC before and after a 50 h open circuit relaxation. The spectra were measured using two different photon energies of 1487 eV and 2984 eV from Al  $K\alpha$  and Ag  $L\alpha$  sources, respectively.



species were detected in the SEI formed in KPF<sub>6</sub>-EC:DEC compared to the SEI formed in NaPF<sub>6</sub>-EC:DEC. C 1s spectra of the SEI formed in KPF<sub>6</sub> electrolyte measured by photon energy of 1487 eV show that the carbonate and carboxyl species diminish after the 50 h pause, indicating their dissolution into the electrolyte. However, a probe of the SEI in the K-system to a greater depth using a photon energy of 2984 eV reveals less compositional changes after the pause, suggesting that while the upper SEI layer undergoes significant alterations, the lower layers remain largely intact. This trend is visible in the red vs. black curves in C 1s, O 1s, F 1s, and P 2p spectra of the K-system measured by the Ag L $\alpha$  source (2984 eV). The C 1s spectra of the Na-system show a slight change in the relative intensity of carbonate and carboxyl peaks, with a more noticeable change in the hydrocarbon peak in the deeper part of the SEI layer. The K 2p peaks observed at the relatively high binding energies in C 1s spectra originate from the presence of KPF<sub>6</sub> and organic potassium containing species.<sup>15</sup>

Additionally, F 1s spectra show that the peak originated from NaPF<sub>6</sub> at approximately 687.5–688 eV remains unchanged after the 50 h pause, whereas the intensity of the KPF<sub>6</sub> peak decreases at the upper part of SEI but remains unchanged at the lower part. This indicates that electrolyte salt species are dissolving from the top surface of the SEI in KPF<sub>6</sub>-EC:DEC. A similar trend could be observed in P 2P spectra revealing that the upper part SEI formed in KPF<sub>6</sub>-EC:DEC undergoes changes during the pause indicating more dissolution of SEI species in K system. However, both F 1s and P 2p spectra of Na system, measured with a photon energy of 1487 eV, show low-intensity peaks at relatively higher binding energies, *i.e.* around 693 eV and 144 eV, which disappear after the pause. These peculiar peaks were likely caused by binding energy shifts induced by surface charging. Also, the changes in the Na KLL Auger peak are likely attributable to surface-charge-induced binding energy shifts.

Overall, the XPS spectra of the SEI in both systems reveal compositional changes arising from the dissolution of various species of the SEI. However, these effects are more pronounced in the SEI formed in the K-based electrolyte, indicating its relatively lower chemical stability and higher solubility compared to that in the Na system.

## Conclusion

The SEI formed in 1 M KPF<sub>6</sub> in EC:DEC on an inert substrate is notably less stable during open circuit storage than that formed in 1 M NaPF<sub>6</sub> in EC:DEC. The sodium-based electrolyte requires 60% less charge consumption for the SEI formation and 50% less for the reformation after a 50 h open circuit pause. The lower stability is attributed to the higher dissolution of SEI species in K-based electrolyte, as confirmed by NMR and XPS analyses. Post mortem <sup>1</sup>H NMR results show the formation of Na/K ethylene di-carbonate and diethyl 2,5-dioxahexanedioate in the electrolyte solutions. XPS results indicate that the inorganic species of the SEI formed in the Na-based electrolyte

remain almost intact during storage, whereas both inorganic and organic species of the SEI formed in the K-system undergo dissolution. The lower stability of the SEI in K-based electrolyte will lead to higher self-discharge rate in potassium battery cells. While this study focuses on PF<sub>6</sub>-based electrolytes containing EC:DEC, the methodology can be broadly applied to investigate SEI ageing mechanisms in sodium- and potassium-ion batteries, facilitating the development of optimized electrolyte formulations for each system.

## Author contributions

J. F. S. writing, review and edit, visualization, formal analysis. L. A. M. conceptualization, writing original draft, investigation (XPS and electrochemistry), visualization, formal analysis. C. A. O. writing, review and edit, investigation (NMR), formal analysis. C. P. G. conceptualization, review and edit. R. Y. conceptualization, writing, review and edit, funding acquisition, project administration.

## Conflicts of interest

Authors declare no conflict of interest.

## Data availability

The data supporting this article have been included as part of the supplementary information (SI). Supplementary information is available. See DOI: <https://doi.org/10.1039/d5ya00173k>.

## Acknowledgements

The authors would like to acknowledge the financial support from ÅForsk Foundation *via* grant no. 20-675 and from the Swedish Energy Agency *via* STandUP for Energy.

## References

- 1 Y. Gao, Q. Yu, H. Yang, J. Zhang and W. Wang, *Adv. Mater.*, 2024, **36**, e2405989.
- 2 S. J. An, J. Li, C. Daniel, D. Mohanty, S. Nagpure and D. L. Wood, *Carbon*, 2016, **105**, 52–76.
- 3 L. A. Ma, A. Buckel, A. Hofmann, L. Nyholm and R. Younesi, *Adv. Sci.*, 2024, **11**, 2306771.
- 4 H. Wang, D. Zhai and F. Kang, *Energy Environ. Sci.*, 2020, **13**, 4583–4608.
- 5 M. Moshkovich, Y. Gofer and D. Aurbach, *J. Electrochem. Soc.*, 2001, **148**, E155.
- 6 L. A. Ma, A. J. Naylor, L. Nyholm and R. Younesi, *Angew. Chem.*, 2021, **133**, 4905–4913.
- 7 M. Martins, D. Haering, J. G. Connell, H. Wan, K. L. Svane, B. Genorio, P. Farinazzo Bergamo Dias Martins, P. P. Lopes, B. Gould, F. Maglia, R. Jung, V. Stamenkovic, I. E. Castelli, N. M. Markovic, J. Rossmeisl and D. Strmcnik, *ACS Catal.*, 2023, **13**, 9289–9301.



- 8 S. Komaba, T. Hasegawa, M. Dahbi and K. Kubota, *Electrochem. Commun.*, 2015, **60**, 172–175.
- 9 J. R. Fitzpatrick, B. E. Murdock, P. K. Thakur, T.-L. Lee, S. Fearn, A. J. Naylor, D. Biswas and N. Tapia-Ruiz, *Adv. Sci.*, 2025, **12**, e04717.
- 10 F. Allgayer, J. Maibach and F. Jeschull, *ACS Appl. Energy Mater.*, 2022, **5**, 1136–1148.
- 11 B. L. D. Rinkel, D. S. Hall, I. Temprano and C. P. Grey, *J. Am. Chem. Soc.*, 2020, **142**, 15058–15074.
- 12 G. V. Zhuang, K. Xu, H. Yang, T. R. Jow and P. N. Ross, *J. Phys. Chem. B*, 2005, **109**, 17567–17573.
- 13 A. Hofmann, F. Müller, S. Schöner and F. Jeschull, *Batteries Supercaps*, 2023, **6**, e202300325.
- 14 J. Nanda, G. Yang, T. Hou, D. N. Voylov, X. Li, R. E. Ruther, M. Naguib, K. Persson, G. M. Veith and A. P. Sokolov, *Joule*, 2019, **3**, 2001–2019.
- 15 L. Caracciolo, L. Madec, G. Gachot and H. Martinez, *ACS Appl. Energy Mater.*, 2021, **13**, 57505–57513.

